Università degli Studi di Padova

Padua Research Archive - Institutional Repository

Finite element simulation of semi-finishing turning of Electron Beam Melted Ti6Al4V under dry and cryogenic cooling

(Article begins on next page)

15th CIRP Conference on Modelling of Machining Operations

Finite element simulation of semi-finishing turning of Electron Beam Melted Ti6Al4V under dry and cryogenic cooling

A. Bordin[a],*, S. Imbrogno[b], G. Rotella[b], S. Bruschi[a], A. Ghiotti[a], D. Umbrello[b]

[a]*Department of Industrial Engineering, University of Padova, Via Venezia 1, 35131, Padova, Italy*
[b]*Department of Mechanical, Energy and Management Engineering, University of Calabria, 87036, Rende (CS), Italy*

* Corresponding author. Tel.: +39 049 8276819; fax: +39 049 8276816. E-mail address: bordin.alberto.dii@gmail.com

Abstract

In the last few years, important step forwards have been made on Finite Element Simulation of machining operations. Wrought *Ti6Al4V* alloy has been deeply investigated both numerically and experimentally due to its wide application in the industry. Recently, Additive Manufacturing technologies as the Electron Beam Melting and the Direct Melting Laser Sintering are more and more employed in the production of biomedical and aeronautical components made of *Ti6Al4V* alloy. Fine acicular microstructures are generated by the application of additive manufacturing technologies, affecting the mechanical properties and the machinability. By the consequence, this peculiarity has to be considered in modelling the material behaviour. In this work, a numerical analysis of cylindrical external turning on Electron Beam Melted (EBM) *Ti6Al4V* alloy is presented. A Johnson-Cook constitutive equation was implemented as a flow stress model and adapted with respect to the wrought Ti6Al4V alloy. The model was calibrated and validated through the cutting forces and temperatures measurements acquired under dry and cryogenic lubricating conditions.

1. Introduction

In the recent years, the diffusion of Additive Manufacturing (AM) technologies is revolutionizing the manufacturing processes of high-tech metallic and polymeric products. More and more companies operating in the aerospace and biomedical fields are revising their manufacturing strategies to produce aero-engine parts and artificial human replacements, "printing" the solid component via powder route instead of passing through the traditional process chains, including casting – hot working – and machining operations. In this way, even complex shapes are built in fewer manufacturing stages. Both the aeronautic and biomedical fields involve a great usage of Titanium alloys and the Ti6Al4V is the workhorse. AM components made of Ti6Al4V are mainly realized by Electron Beam Melting (EBM), Direct Melting Laser Sintering (DMLS), and Selective Laser Melting (SLS) techniques. By

these forming processes, the alloy microstructure is strongly influenced, in particular finer microstructures are obtained in comparison with the ones of the hot worked or casted Ti6Al4V alloys [1], hence different mechanical properties result. Even though the adoption of AM techniques in manufacturing metal components reduces drastically the amount of machining operations, finishing milling and turning operations are still required to remove the porous surface layers, to compensate the geometrical inaccuracies of the process itself, and to prepare the surfaces to be joined with other components as the polymeric and ceramic inserts. Based on these considerations, with the aim of optimizing the production process chain and moreover respecting the surface integrity requirements, the machinability of the material must be properly investigated. Several works have been conducted during the years aimed at

improving the machinability of the wrought Ti6Al4V through both numerical and experimental techniques, whereas no exhaustive works are available for the AM titanium alloys. Finite element analysis of metal cutting operations are gaining more and more attention in the scientific community, foreseeing the possibility of predicting even complex thermo-mechanical phenomenon as the induced residual stresses and the microstructural alterations [2, 3]. Considering the numerical simulation of metal forming processes, a key factor is the availability of a validated material model equation. In the case of the wrought Ti6Al4V, the Johnson–Cook (JC) material model is widely adopted to predict the material flow behaviour, and some modifications were implemented to better simulate the material behavior as a function of the temperature, strain and strain rate, such as in the Calamaz [4] and zel [5] models. However, none of the works available in literature about FEA of machining processes deals with AM titanium alloys. The present work is aimed at developing the numerical simulation of machining operations conducted on the EBM Ti6Al4V alloy under semi-finishing cutting conditions. A JC based constitutive model was properly adapted and implemented into a commercial FE code. Semi-finishing turning tests carried out with adopting three levels of cutting speed and two levels of feed rate under dry and cryogenic lubricating conditions were employed to calibrate and validate the numerical model by comparing the cutting forces and temperatures.

2. Experimental procedure

2.1. Material

The machining tests were performed on the EBM Ti6Al4V supplied in the as-built condition, without any post forming heat treatment, according to the industrial standard. The microstructural analysis of the as-built material revealed a fine acicular microstructure that is clearly visible in Fig. 1: a basket wave morphology of α phase lamellae is visible as the white phase, while the dark lamellae corresponds to the β phase that typically is present in a percentage from 5 to 10. This microstructure is the consequence of the rapid solidification after the local melting of the metal powder and the following stabilization at the forming temperature of 600°C. Even though negligible variations are present in the chemical composition between the wrought and EBM alloys [1], a general increment of the UTS and hardness in the case of the AM alloy as indicated in Table 1 induces a worse machinability as found in [6]. The tested material was supplied in bars, which were grown having their symmetrical axis parallel to the electron

Table 1. Mechanical properties of the EBM Ti6Al4V (as-built condition) compared with the ones of the wrought alloy (ASTM F1472).

Material	E [GPa]	UTS [MPa]	YS [MPa]	Elongation [%]	HRC
EBM Ti6Al4V	114	914	830	13.1	35
Wrought Ti6Al4V	118	872	790	16	31

beam direction. The test pieces presented a diameter of 50 mm and length of 160 mm. In order to remove the porous surface layer that is generated by the EBM technique, the bars were pre-turned to a diameter of 49 mm before the experimental campaign.
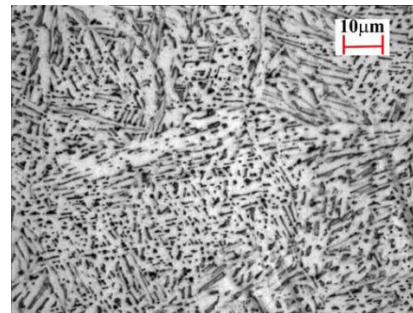

Fig.1. Microstructure of the EBM Ti6Al4V in the as-built condition.

2.2. Machining tests set-up

The semi-finishing turning tests were conducted on a Mori Seiki NL 1500 CNC lathe, equipped with a system aimed at supplying the Liquid Nitrogen (LN2) directly to the cutting zone. The LN2 is carried through a vacuum insulated pipe and a nozzles system composed by two cooper nozzles with an internal diameter of 0.9 mm that direct the flow towards the tool rake face and the primary cutting edge with an inclination of 45°. The utilized cutting tool inserts were uncoated carbide, Sandvik Coromant® CNMG 120404-23 H13A, mounted on a PCLNR/L 2020k12 tool holder supplied by the same manufacturer. The effective cutting angles and the tools geometry were measured with a Sensofar Plu-Neox™ optical profiler by scanning the tool insert mounted on the tool holder. The effective cutting angles resulted of being equal to 7° and 8° for the rake and clearance angles respectively, while an approaching angle of 95° is defined by the tool holder geometry. A fresh cutting edge was adopted for each cryogenic and dry turning test, thus neglecting the tool wear effect in such short turning lengths. The turning trials, aimed at calibrating and validating the numerical model, were six for each lubricating conditions, resulting by the combination of three values of cutting speed and two values of feed rate, namely 50, 80 and 110 m/min, and 0.1 and 0.2 mm/rev, respectively; the depth of cut was kept constant and equal to 0.2 mm in order to respect the semi-finishing turning conditions. The turning length was calculated for each turning trial ensuring a minimum machining time of 20 seconds to reach a steady state condition for the cutting temperature and forces. The experimental set up for the machining tests is shown in Fig. 2, in which the instruments adopted for the in-line acquisitions of the cutting variables are shown. A Kistler®- type 9257 B three components piezoelectric dynamometer was mounted on the lathe revolver for the acquisition of the cutting forces along the cutting speed and feed directions. An infrared camera FLIR A6000-series was fixed on the tailstock allowing the acquisition of the thermal field from a frontal position with regard to the workpice.
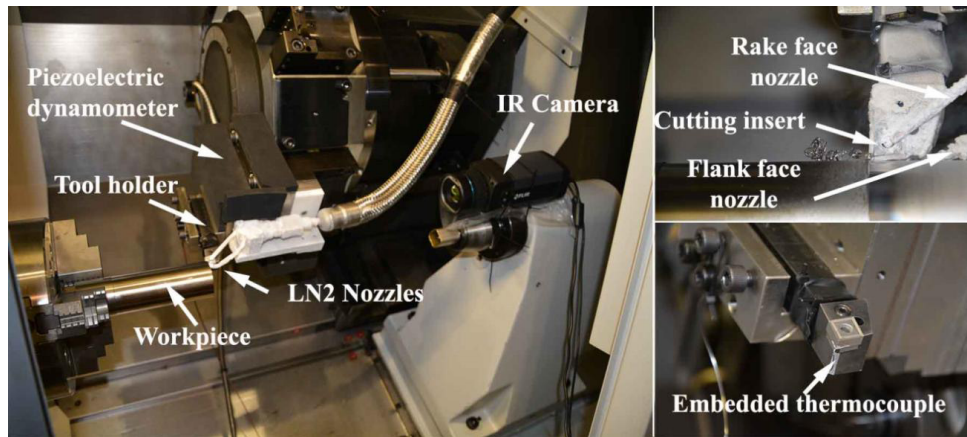
Fig. 2. Experimental setup for cryogenic machining.

The material emissivity calibration was realised by heating up a test piece into a temperature-controlled electrical furnace. The temperature near the cutting zone was measured thanks to a 0.5 mm diameter thermocouple embedded into the turning insert: a T-type thermocouple was employed for the cryogenic cooling conditions, while a K-type one for dry turning. In both cases, a hole of 0.9 mm diameter and 3 mm depth was realized by EDM at a distance from the tool nose of 1 mm. The thermocouple was maintained fixed in position during the machining operation by a thermo-conductive bound deposed into the hole, filling all the cavities. The acquisition of the cutting temperatures and forces was achieved by a LabView® based software.

3. FE Numerical procedure

The proposed numerical procedure developed in this paper is aimed at testing the feasibility of a consolidated material constitutive model for the wrought Ti6Al4V when implemented in a 3D FE model of a turning operation conducted on the EBM Ti6Al4V under dry and cryogenic conditions. Most of the material constitutive models for simulating the thermo-mechanical behavior of the wrought Ti6Al4V are based on the renowned J-C flow stress rule [7-9]. Based on previous works about Ti6Al4V machining simulation [10], the J-C material model modified by zel in [11] was implemented into the numerical model. This modified material model proved its capability of predicting the chip morphology and cutting forces more accurately than the classic Johnson-Cook model coupled with a damage criterion, such as the Cockroft and Latham, Brozzo ones [12]. More in detail, the flow softening, which is believed to cause adiabatic shearing within the primary shear zone and thus the Ti6Al4V chip segmentation during machining operations, is mathematically modelled by additional terms to account for the strain softening effect dependent on the equivalent strain.

An accurate description of the singular parameters of the flow stress model and their physical meaning can be found in dedicated published works [11], nonetheless the equations implemented in the model can be written as:

$$\sigma = \left[A + B\varepsilon^{n} \right] \left[1 + C \ln \frac{\dot{\varepsilon}}{\varepsilon 0} \right] \left[1 - \left(\frac{T - Tr}{Tm - Tr} \right)^{m} \right]$$

$$\left[D + (1 - D) \left[\tanh \left(\frac{1}{(\varepsilon + P)^{r}} \right) \right]^{s} \right] \tag{1}$$

$$D = 1 - \frac{T}{Tm} \tag{2}$$

$$P = \left(\frac{T}{Tm} \right)^{s} \tag{3}$$

where the constants A, B, C, n and m are listed in the Lee Lin work [13], while r and S are the material parameters introduced by zel [14]. The room temperature T_r was set equal to 20° for both dry and cryogenic cooling.

The assumption of implementing a flow stress model that has demonstrated accurate numerical predictions in 2D and 3D turning of the wrought Ti6Al4V was considered by evaluating the tiny differences in terms of chemical composition and mechanical properties between the EBM and wrought alloys as evidenced in Table 1. Moreover, a previous experimental work conducted by [6] on a comparison between the cutting conditions highlighted the occurrence of the same chip segmentation and tool wear mechanisms for both the alloys.

The commercial FEA code SFTC Deform 3D® was utilized to simulate the semi-finishing turning operation. The cutting tool was modeled as a rigid body (divided into 38000 elements), and an isotropic hardening was assumed for the material of the workpiece, which was divided into 85000 elements. Regarding the mesh density, the elements around the tool nose and along the machined surface were fifty times as dense as the other ones that presented a length of 7 μm.

The cutting tool and the workpiece were allowed exchanging heat with the environment, by setting a convection

coefficient equal to 20 W/(m²K), which is a standard value for free-air convection in DEFORM, whereas an environmental window for heat exchange was defined between the machined surface and the flank side of the tool, near the tool radius to simulate cryogenic cooling effect, by setting a local temperature of -196°C and a convection coefficient, namely h_{cryo}. As demonstrated in a previous work [10, 12], a good agreement between measured and predicted temperatures under cryogenic cooling is achieved for a value of h_{cryo} equal to 20 kW/(m²/K). Aiming at reaching a thermal steady state condition at the tool chip interface in a short computational time, with the assumption of a thermally perfect contact, a global heat transfer, h_{int}, was set equal to 100000 kW/(m²/K), according to the literature results [9]. Finally a sticking-sliding friction model (sticking governed by the shear model $\tau = m\tau_0$; sliding governed by the Coulomb model $\tau = \mu\sigma$) was also implemented; the friction coefficients m and μ were chosen equal to 0.8 and 0.9, respectively, according to [12].

3.1. FE calibration

The calibration of the FE model consisted in computing the friction coefficients that characterizes the implemented sticking - sliding friction model, namely m for the sticking friction and μ for the sliding friction. Furthermore, even the coefficient A of the J-C equation (see eq. (1)), that governs the YS exhibited by the Ti6Al4V alloy, was calibrated to better fit the higher mechanical properties of the EBM Ti6Al4V in comparison with the wrought one (see Table 1). Based on recent works devoted at measuring the friction coefficients when machining under cryogenic cooling, the adoption of LN2 provokes a variation on the friction mechanisms, hence on the friction coefficients. According to that, two parallel calibration procedures were performed to evaluate the friction coefficients, while the coefficient A was computed under dry condition. The calibration procedure was carried out for two cutting conditions tested, corresponding to the following cutting parameters: cutting speed of 50 m/min and feed rate of 0.1 mm/rev for the first condition, and cutting speed of 110 m/min and feed rate of 0.2 mm/rev for the second one. An iterative inverse analysis was implemented, based on error minimization by comparing experimental and predicted results
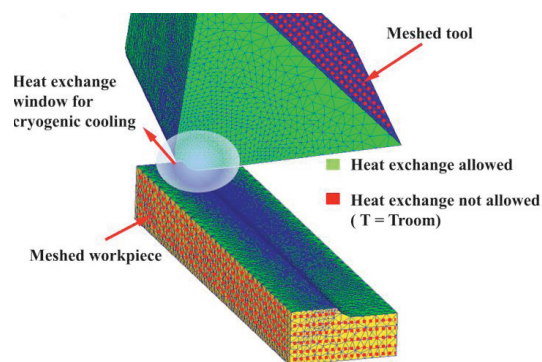

Fig. 3. FE model and thermal assumption for simulating cryogenic cooling.

of the main cutting force Fc, fixing a threshold value of 10% as an acceptable error. At the end of the calibration procedure, the friction coefficients resulted of being equal to 0.2 and 0.3 for μ and m respectively, whereas on the other side higher values resulted under cryogenic cooling being equal to 0.3 and 0.4. The coefficient A of the J-C equation was raised to 940MPa instead of the initial value assumed equal to 724.7 MPa.

4. FE Validation and FE analysis

After the calibration phase, the FE model was validated by comparing the experimental results and the corresponding numerical data. FE simulations were executed for all the tested turning trials, the average values of the cutting forces were then calculated when a steady state condition was reached. Figure 4 shows the comparison between the measured and predicted cutting forces for dry and cryogenic machining. The predicted main cutting force fits correctly the experimental data for all the tested cutting condition under both dry and cryogenic cooling conditions. The highest errors were equal to -8.7 and -6.8 % for dry and cryogenic cooling conditions, respectively, when, in both the cases, the more severe cutting parameters were adopted, namely cutting speed equal to 110 m/min and feed rate equal to 0.2 mm/rev. Figures 6 and 7 show that even the feed force trend is correctly predicted although the differences between predicted and experimental data are higher than for the main cutting force. These discrepancies might be related to the used friction models that are well validated for orthogonal machining but not yet for 3D machining. More in detail, other important parameters might be taken into account and related to the friction coefficient as the tool geometry (tool nose radius, angles, etc.) and the grain size. It is worth to point out that for both the components of the cutting force, a progressive decrement is observed at increasing the cutting speed for the tested lubricating conditions. This aspect might be related to the thermal softening of the Ti6Al4V alloy that is provoked by the major heat generated into the cutting zone when increasing the cutting speed.

Another important variable considered in validating the numerical model was the cutting temperature. The comparison between the measured and predicted cutting temperatures is showed in Fig.5, in which the cutting temperature measured by means of the IR Camera is compared with the average value computed on the tool rake face. The FE model simulates correctly the trend of the cutting temperatures at varying the cutting speed for both lubricating conditions tested even dough some discrepancies are denoted and the numerical and the experimental values. It is worth to note that the discrepancies might be partially induced by the high sensitivity of the temperature measurements with the selected position on the FE model and on the IR image. Nonetheless, the proposed model predict correctly the increasing trend of the temperature with the cutting speed for both dry and cryogenic conditions.

Figure 6 on the right shows a coloured FE map representing the spatial distribution of the strain in the portion of material being cut along the radial direction.
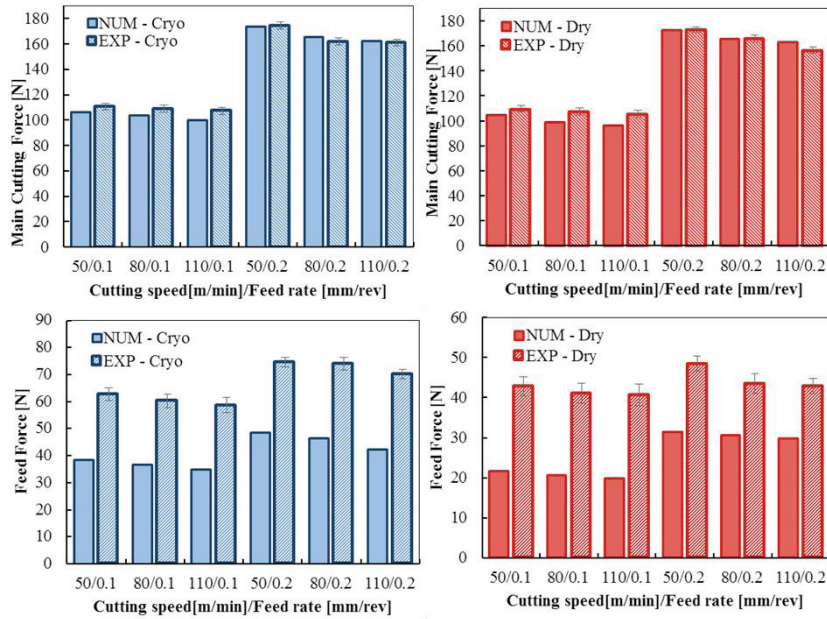
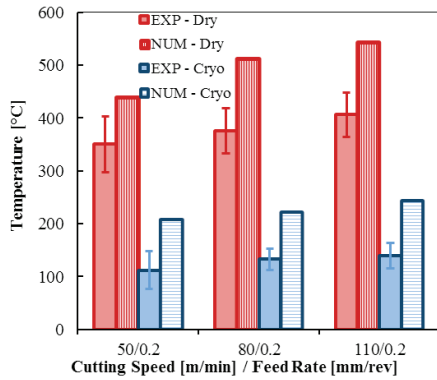Fig.4. Comparison between measured and predicted main cutting forces during dry and cryogenic machining.

Fig 5. Comparison between the predicted and measured cutting temperatures.

The model predicts correctly the strain gradient along the radial direction in the portion of the material being cut under the tool nose, indicated as the valid zone in Fig.6.

It is of fundamental importance to underline that only the portion of the FE model that presents the correct mesh setting can be considered for evaluating the numerical results, being the portion not totally affected by the remeshing steps. One of the main parameters to consider when evaluating the effects of machining operations on the material is the thickness of the severe plastic deformation layer, namely SPD as indicated in Fig.7. The average thickness of the SPD layer was evaluated in three different positions into the as defined valid zone. The proposed FE model predicts correctly the trends of the SPD thickness, where an increment is observed when increasing the cutting speed, moreover higher values of SPD are found when adopting the cryogenic cooling.

5. Conclusions

This paper presents a FE model of semi-finishing turning operation carried out on EBM Ti6Al4V under dry and cryogenic cooling conditions. Due to the lack of literature works and material properties, a modified Johnson-Cook model validated for the wrought Ti6Al4V was implemented and coupled with an hybrid sticking – sliding friction model for modelling the friction forces on the cutting tool.

The model was calibrated and validated by comparing the predicted main cutting force with the experimental one under a couple of cutting conditions.
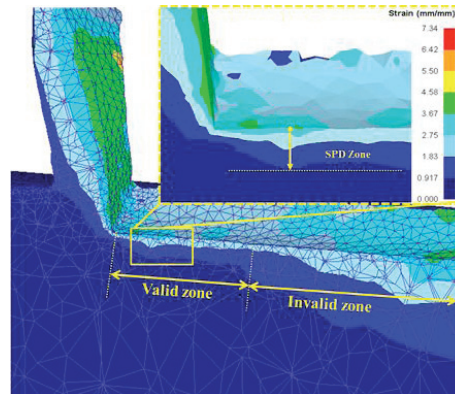

Fig. 6. Map of strain distribution during FEA simulation along the radial direction under the machined surface.
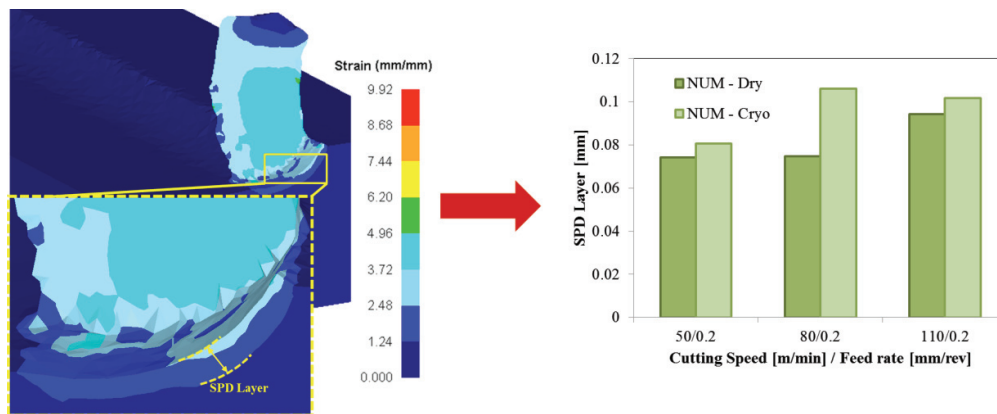
Fig.7. Position of the severe plastic deformation layer (SPD) in the FE model on the right. Average SPD layer thickness on the left.

The numerical results show a very good prediction of the main cutting force for all the tested cutting conditions under dry and cryogenic machining. The predicted feed force shows a trend that respects the experimental findings but wider discrepancies between the values are present, mainly due to the friction model that should be validated for 3D turning operations. Furthermore, the FE model predicts correctly the trends of importance parameter to evaluate when investigating the machinability of a material as the SPD layer thickness under the machined surface and the cutting temperature.

References

[1] Facchini L., Magalini E., Robotti P., Molinari A., Microstructure and mechanical properties of Ti-6Al-4V produced by Electron Beam Melting of pre-alloyed powders. Rapid Prototyping Journal15/3 (2009) 171.

[2] Pu Z., Umbrello D., Dillon Jr.O.W., Jawahir I.S., Finite Element Simulation of Residual Stresses in Cryogenic Machining of AZ31B Mg Alloy. Procedia CIRP 13 (2014) 2014 282-287.

[3] Umbrello D., Outeiro J.C., M'Saoubi R., Jayal A.D., Jawahir I.S., A numerical model incorporating the microstructure alteration for predicting residual stresses in hard machining of AISI 52100 steel. CIRP Annals - Manufacturing Technology 59(1)(2010) 113-116.

[4] M. Calamaz, Etude des me´canismes d'endommagement des outils carbure WC-Co par la caracterisation de l'interface outil-copeau—Application a l'usinage de l'alliage de titane aeronautique TA6V''. Ph.D. Thesis, Universite´de Bordeaux, France, No. 2008-3605, June 2008.

[5] Özel T., Sima M., Srivastava A.K., Kaftanoglu B., Investigations on the effects of multi-layered coated inserts in machining Ti-6Al-4V alloy with experiments and finite element simulations. CIRP Annals of Manufacturing Technology 59 (1) (2010) 77–82.

[6] Bordin A., Comparison between Wrought and EBM Ti6Al4V Machinability Characteristics. Key Engineering Materials 611- 612 (2014) 1186-1193.

[7] Johnson G.-R., Cook W.-H., A constitutive model for metals subjected to large strains, high strain rates and high temperatures, in: Proceedings of the Seventh International Symposium on Ballistics, Hague, Netherlands, vol. 54,1983, pp. 1–7.

[8] Shrot A., Bäker M., Determination of Johnson–Cook parameters from machining simulations. Computational Materials Science 52 (1) (2012) 298-304.

[9] Umbrello D., M'Saoubi R., Outeiro J.C., The influence of Johnson–Cook material constants on finite element simulation of machining of AISI 316L steel. International Journal of Machine Tools and Manufacture 47 (3–4) (2007) 462-470.

[10] Pu Z., Umbrello D., Dillon Jr. O.W., Jawahir I.S., Finite Element Simulation of Residual Stresses in Cryogenic Machining of AZ31B Mg Alloy. Procedia CIRP (13) (2014) 282-287.

[11] Sima M, Özel T., Modified material constitutive models for serrated chip formation simulations and experimental validation in machining of titanium alloy Ti–6Al–4V. International Journal of Machine Tools and Manufacture 50 (11) (2010) 943-960.

[12] Rotella G., Umbrello D., Finite element modelling of microstructural changes in dry and cryogenic cutting of Ti6Al4V alloy. CIRP Annals - Manufacturing Technology 63 (1) (2014) 69-72.

[13] Lee W. S., Lin C. F., Plastic deformation and fracture behaviour o Ti–6Al–4V alloy loaded with high strain rate under various temperatures. Mater. Sci. and Eng. A 241 (1998) 48–59.

[14] Özel T., Sima M., Srivastava A.K., Kaftanoglu B., Investigations on the effects of multi-layered coated inserts in machining Ti-6Al-4V alloy with experiments and finite element simulations, CIRP Annals of Manufacturing Technology, 59 (1) (2010) 77–82.